ARTICLE

Iron Based Nano-structures' Surface with Antimicrobial Property

Guangshun Yi,*[a] Siew Ping Teong,[a] Shaoqiong Liu,[a] Shuyun Chng,[b] Yi Yan Yang[a] and Yugen Zhang*[a]

Received 00th January 20xx,
Accepted 00th January 20xx

DOI: 10.1039/x0xx00000x

Bactericidal nanopillar arrays on cicada wings represent a non-toxic antimicrobial technology as it works through physical cell rupture instead of chemical components. Here we reported an iron-based nanopillar arrays (FeOOH and Fe_2O_3) which can grow on various substrates by a simple solution method. These surfaces showed good structure-based antimicrobial activity. Even more simply, we have prepared urchin-type FeOOH and Fe_2O_3 particles which can be easily coated onto various substrates to create structure-based disinfection surfaces. This work provides a simple and general methodology to apply this killed-by-structure technology for real world uses.

1. Introduction

Over the course of human history, pathogens (bacteria and virus) are among the top threats to human lives, until the discovery of antibiotics and vaccines.[1] However, bacteria have quickly developed resistance against almost all type of antibiotics. Antimicrobial resistance (AMR) has now become one of the most critical challenges in our modern society.[2, 3] One of the major causes of AMR development is the unnecessary use of antibiotics in areas such as non-therapeutic applications in environmental disinfection.[4] The accumulation of low levels of antimicrobial materials in the eco-system over long periods of time led to the selection of drug resistance microbes.[4] On the other hand, up to 80% of the pathogens are transmitted through surface contact.[5] Thus, the eradication of microbes on frequently contacted surfaces is an effective strategy to avoid cross infections.[6, 7] The challenge here is to have disinfected surfaces without using any antibiotics or chemical disinfectants.

In response to this threat of drug resistance and the rising demand for self-disinfecting surfaces, microtopographic surfaces have attracted much attention as they represent a green antimicrobial strategy to replace biocides.[8-11] In the early stages, artificial nanopatterned surfaces mimicking lotus leaves and other natural surfaces have been made for self-cleaning and anti-biofouling applications.[12-16] More recently, natural surfaces such as cicada wings and dragonfly wings were discovered to have bactericidal properties.[17-19] This represents a promising discovery as further studies showed that the antibacterial effect was purely based on physical rupture instead of chemical composition.[20-22] This opens up a great opportunity for the development of innovative microbicide surfaces which are clean and safe, require no external chemicals, and are theoretically hard to develop resistance.[23] However, making this type of nanostructures on common surfaces with simple methods remains a big challenge.

In recent years, many man-made nanotopographies mimicking cicada wings have been reported with bactericidal properties.[24-29] For example, nanostructured surface of of Si,[24, 30, 31] TiO_2,[25, 32, 33] ZnO,[34, 35] polymer,[26, 36, 37] SiO_2,[27] ZIF-L MOF,[38] Au,[39] and stainless steel,[40] have been prepared and reported to have structure-based antibacterial properties. However, most of the methods used for fabricating surface nanopatterns encountered issues of requiring special equipment,[24, 26, 31] expensive starting materials,[24, 30, 31] and are only specific to certain substrates etc.[22, 24, 25, 27, 29, 30, 33] It is critical to develop a simple and scalable method to create the biocidal nanostructure on commonly used substrates for practical applications.[34, 38] So far only a few reported method can grow bactericidal nanostructures on various commonly used substrates. For example, the ZnO nanopillars reported by our group[34] and Xie et al,[35] and ZIF-L coating reported by us can grow on many substrates.[30] However, more efforts are still required to develop a simple method to apply this structure-based antimicrobial technology on any surfaces.

An ideal microbicide nanopillars surface should have the following features: easy preparation, readily available, non-toxic starting materials, and good antimicrobial properties. Iron is the 4th most abundant element (5%) after O, Si and Al on earth, and iron oxide (e.g. goethite and hematite) is clearly environmentally benign.[41] Goethite (β-FeOOH) has existed on earth for billions of years and is widely used as a pigment (brown ochre). Hematite (α-Fe_2O_3) is one of the richest minerals on earth and it is the main source of steel smelting. Hematite is also widely used as a red pigment.[41] Herein, FeOOH nanopillars have been growing on glass and other various surfaces which demonstrate microbicidal properties. The FeOOH pillars surface can be easily converted to α-Fe_2O_3 by a simple heat treament without affecting their original structures.

[a] *Institute of Bioengineering and Nanotechnology, 31 Biopolis Way, The Nanos, Singapore 138669, Singapore. Email: gsyi@ibn.a-star.edu.sg; ygzhang@ibn.a-star.edu.sg.*
[b] *Singapore Institute of Manufacturing Technology, 2 Fusionopolis Way, #08-04, Innovis, Singapore 13863*
† *Electronic Supplementary Information (ESI) available. See DOI: 10.1039/x0xx00000x*

Furthermore, we have also reported a method to prepare sea urchin type FeOOH and Fe_2O_3 particles. By simply coating these particles together with binder onto a substrate, the nanopillars surface is built, with good antimicrobial properties. These self-standing nanostructures provide a simple and general methodology for the realistic application of the structure-based antimicrobial technology.

2. Experimental section

2.1 Chemicals and Materials

$FeCl_3.6H_2O$, Na_2SO_4 and FTO glass were purchased from Sigma-Aldrich. Microscope slides (76 × 26 × 1 mm) were purchased from MARIENFELD, Germany. Tryptic soy broth (TSB) and yeast mould broth (YMB) powder were purchased from BD Diagnostics (Singapore) and used to prepare the broths according to the manufacturer's instructions. Gram-negative bacteria *E. coli* (ATCC No. 8739), Gram-positive bacteria *S. aureus* (ATCC No. 6538P), and fungi *C. albicans* (ATCC No. 10231) were purchased from ATCC (U.S.A) and re-cultured according to the suggested protocols.

2.2 Instrumentation and characterization

The surfaces of the samples were characterized by SEM (JEOL JSM-7400E), and XRD (PANalytical X-ray diffractometer, X'pert PRO, with Cu Kα radiation at 1.5406 Å). Prior to SEM, the samples were coated with thin Pt film using high resolution sputter coater (JEOL, JFC-1600 Auto Fine Coater). Coating conditions: (20 mA, 30 s). LIVE/DEAD images were taken on Fluorescence microscope (Zeiss LSM-510 confocal fluorescent microscope, and Olympus inverted microscope, 1X71).

2.3 Sample preparation

Preparation of FeOOH and Fe_2O_3 nanopillar array on surfaces. An aqueous solution of $FeCl_3.6H_2O$ (0.946 g), Na_2SO_4 (0.479 g) in water (70 ml) was placed into a 100 ml hydrothermal reactor. The substrate surface (glass, FTO glass, tin-plated steel or Teflon) was washed with a solution of i-PrOH/H2O/Acetone (1:1:1) and placed into the hydrothermal reactor with the growing surface facing down. The reactor was heated to 100 °C for a certain time from 6-24 h. After that, yellowish colored FeOOH nanopillars array were fabricated on the surface. The surface was then washed with deionized water and ethanol and dried in ambient air.

To convert the FeOOH into Fe_2O_3 nanopillars, the FTO glass and tin-plated steel with FeOOH nanopillars on surface were placed into a furnace and heated to 500 °C for 3 h. The yellowish FeOOH nanopillars on surface were then converted to red Fe_2O_3 nanopillars.

Preparation of FeOOH nanopillar on FTO glass. Same procedure as described above but change the reaction temperature to 120 °C for 24 h.

Preparation of FeOOH and Fe_2O_3 sea urchin-like particles. An aqueous solution of $FeCl_3.6H_2O$ (0.946 g), Na_2SO_4 (0.479 g) in water (70 ml) was placed into a 100 ml hydrothermal reactor. The reactor was sealed and placed into an oven preheated at 100 °C and allowed to react for 24 h. After cooling down, the particles were collected by centrifuge, washed 3 times with DI water and dried in 60 °C oven to obtain the yellowish FeOOH urchin-like powder.

To convert FeOOH to Fe_2O_3 urchin-like particles, the powder was calcined at 500 °C for 3 h. Dark red Fe_2O_3 urchin-like powder was then obtained.

Preparation of FeOOH and Fe_2O_3 urchins coating on surfaces. On a 2.5 cm × 2.5 cm glass slide, FeOOH (2.3 mg) or Fe_2O_3 (1.9 mg) was dispersed in ethanol and coated onto the surface. After drying, the surface was used for JIS testing. The amount of powder used was calculated based on the average weight of nanopillars array growing on 5 glass surfaces.

Preparation of FeOOH and Fe_2O_3 urchin coatings with aqueous-based paint as binder. 1:4 ratio of the powder to Nippon paint (1:5 diluted) was prepared, ultrasonic to homogenous and applied onto glass pieces (2.5cm x 2.5cm). They are further dried in a 60 °C oven overnight before antibacterial testing.

2.4 Biological experiments

Microbe growing conditions and sample preparation. The bacteria were grown in TSB broth overnight in a shaking incubator at 37 ˚C. Fungi *C. albicans* were grown in YMB broth at room temperature. Prior to each bacterial experiment, bacteria were refreshed from each stock in 5 ml respective broth. Bacteria cells were collected at the logarithmic stage of growth.

JIS Z 2801/ISO 22196 method for killing efficacy testing (Japanese industrial standard). Before JIS testing, *E. coli* and *S. aureus* were diluted in 1/500 TSB solution, and *C. albicans* were diluted in 1/100 YMB, and adjusted to OD_{600} = 0.07. This corresponds to 3×10^8 CFU/ml. The solution was further diluted 100 times before 100 µL of cell suspensions was place d on the testing surfaces. After incubation for 24 h, bacteria on the testing surface was washed off with 9.9 ml of pH 7.4 PBS buffer solution, sequentially diluted and plated on 1.5 % LB agar plates. Resulting colonies were counted using standard plate count techniques, and the number of colonies forming units (CFU) per mL was calculated.

Antibacterial testing (droplet method). Bacteria were cultured for 3-5 h in fresh TSB, centrifuged at 3000 rpm for 5 min and re-dispersed in PBS, adjusted to OD_{600} = 0.07. This corresponds to 3×10^8 CFU/ml. The suspension was further diluted in PBS to give a concentration ranging from 2.5×10^6 to 10×10^6 CFU/ml. On each testing surface, 2.5 µl of bacterial solution was dropped, and cultured at room temperature for 0 min, 5 min, 10 min, 15 min and 60 min. After that, the surfaces were washed with 2.5

ml of PBS buffer solution. 100 ul of solution was spread onto an agar plate and cultured at 37 °C overnight before plate counting.

SEM imaging. Bacteria concentration was adjusted to OD_{600}=0.07 in 1/500 TSB by a microplate reader (TECAN, Switzerland), which corresponded to 3×10^8 CFU/ml. 100 μL of bacteria suspension was added to the testing surface (2.5 cm × 2.5 cm) and incubated at 37 °C (room temperature for *C. albicans*) for 24 hours.

The surfaces were fixed in 2.5% glutaldehyde PBS solution for 2 h, and soaked each sample in 30%, 50%, 70%, 85%, 90%, and 100% ethanol twice. Each concentration was treated for 20 mins. The treated surface was placed in a fume hood and left for 24-48 h, which was further coated with platinum before SEM imaging. The morphologies of the bacteria before and after treatment were observed using a field emission SEM (JEOL JSM-7400F) operated at an accelerating voltage of 10.0 kV and a working distance of 8.0 mm.

LIVE/DEAD fluorescence imaging. Bacteria concentration in 1/500 TSB was adjusted to OD_{600}=0.07 by a microplate reader (TECAN, Switzerland), which corresponded to 3×10^8 CFU/ml. After 10 times dilution with 1/500 TSB, 10 μL of bacteria suspension was added to the surface (1 cm × 1 cm) and incubated at 37 °C for overnight.

The surfaces were dyed with LIVE/DEAD dye (Invitrogen) following the manufacture's protocol, and the image was taken on fluorescence microscope (Zeiss LSM-510 confocal fluorescent microscope, and Olympus inverted microscope, 1x71).

In vitro biocompatibility study (MTT method). L929 cells were cultured in DMEM supplemented with 10% FBS, 5% penicillin, 2 mM L-glutamine (Sigma) and incubated at 37 °C with 5 % CO_2. Glass slides, FeOOH, and Fe_2O_3 nanopillars array surfaces, all cut to 1 cm × 1 cm size, were put in 12 well culture plates (Corning). The cells were seeded onto each well at 100, 000 cells per well and incubated overnight.

After that, the testing surfaces were transferred to a new 12-well plate, and freshly grown media (900 μL) and MTT solution (100 μL) were added to each sample in the wells. The plate was then returned to the incubator and maintained in 5 % CO_2, at 37 °C, for a further 4 h. The growth medium and excess MTT in each well were removed before DMSO (1000 μL) was added to each well to dissolve the internalized purple formazan crystals. An aliquot of 100 μL was taken from each well and transferred to a fresh 96-well plate. Each sample was tested in three replicates per plate. The absorbance reading of the formazan crystals was taken to be that at 550 nm subtracted by that at 690 nm. The results were expressed as a percentage of the absorbance of the blank control.

3. Results and discussion

3.1 Synthesis and Characterization

Growing FeOOH nanopillar arrays on glass substrate was prepared through a simple solution method.[42] A yellowish FeOOH nanopillar film was formed on top of the glass substrate. Figure 1a and 1b show the SEM images of the top-view and tilt-view of the surface respectively. Vertically-aligned FeOOH nanopillar arrays were growing on the glass substrate. The nanopillars have sharp tips with diameters of < 33 nm and lengths of 1.78 ± 0.24 μm. The space between pillars is measured to be 202 ± 55 nm. For comparison, the height of the cicada wing (*P. claripennis*) ~200 nm, dragonfly wing (*D. bipunctata*): ~240 nm, black silicon: ~500 nm.[24] Figure 1c shows the XRD pattern of the product on glass, assigned to the tetragonal β-FeOOH phase according to the JCPDS card number 34-1266, thus confirming the formation of well crystalline β-FeOOH structure.[43]

Besides glass substrate, the growing of FeOOH nanopillar arrays on other substrates has also been studied. These substrates include FTO glass (fluorine-doped tin oxide glass), plastics (Teflon), and metal (tin-plated iron), as showed in Figure 1d-f. All the nanopillars are similar to the ones growing on glass slides. It was found that the nanopillar arrays on FTO glass and tin-plated iron are much stronger than the ones on other substrates. Nanopillar array layers on glass slides and Teflon tape surfaces can be peeled off as a continuous thin film when the substrate bends (Teflon tape, Figure S1a) or by strong air blowing / over drying (glass, Figure S1b). The self-standing nanopillar film retained a good structure—as good as the structure on the supporting substrates. This suggested that the FeOOH nanopillars array was physically adhered to the supporting substrates, instead of adhering to them via chemical bonding. On the other hand, FeOOH nanopillar arrays on FTO glass and tin-plated iron was strong and cannot be peeled off in the same way. Since both FTO glass and tin-plated iron have tin on their surfaces, this may suggested that the nanopillar arrays adhered to these surfaces by chemical bonding of tin-O-iron. The adhesive force of the coatings on glass and FTO glass was measured following the ISO 2409 standard and the testing score is 5 (cannot be classified).

The aspect ratio of nanopillars has direct impact on their antibacterial properties.[44] To control the aspect ratio of the nanopillars, the reaction conditions were studied. Reaction time from 6 h to 24 h has no obvious effect on the height of the pillars. However, the nanopillars became thicker and stronger when the reaction time increased from 6 h to 12 h (Figure S2), and observed no change from 12 h to 24 h. Lowering the reactant concentration to 1/3 produced FeOOH nanopillars with 1/3 length (Figure S3a and Figure 3a). Doubling the reactant concentration did not increase the length of the nanopillars. Instead, a pyramid-shaped FeOOH array with aspect ratio <1 was formed (Figure S3b, S4 and 3c). Hence, a two-step method was proposed to pursue longer pillars. After FeOOH nanopillars grew on the surface at standard conditions, the surface was further placed into another fresh reaction solution with the same reactant as the first step. Although we obtained longer

nanopillars through this method, the FeOOH pillars array had an uneven bump surface, as shown in Figure S5b and Figure 3b.

The growth conditions of FeOOH on FTO glass is slightly different from the conditions for other substrates. On other substrates, the reaction temperature was 100 °C for 12-24 h. The length of each pillar is 1-2 μm. However, on FTO glass, under these conditions, we obtained nanopillars of < 1 μm with a low aspect ratio (Figure S6a). Therefore we increased the reaction temperature to 120 °C for 24 h, which gave a similar structure as the one on the glass substrate (Figure S6b). Raising the temperature to 150 °C for 24 h yielded a dark red coating of Fe_2O_3 on FTO glass. However, this structure was not the desired pillars array surface (Figure S6c).

3.2 Antimicrobial properties

The antibacterial property of the FeOOH nanopillars on FTO glass was first investigated against *E. coli* with the JIS Z 2801/ISO 22196 method.[45] For this test, FeOOH nanopillar arrays growing on FTO glass was used (Figure 2a). For comparison, bare FTO glass and 2.3 mg FeOOH pillar particles (peeled off from glass and grinded gently with mortar to destroy the array) randomly-coated on FTO glass (Figure 2b) were used as control. The average weight of FeOOH growing on each FTO glass was 2.3 mg, determined by weighing 5 pieces of samples before and after reaction. As shown in Figure 2c, no bacterial colony was observed after a 24 hour incubation period, this showed the surfaces are bactericidal rather than anti-fouling. Conversely, no antibacterial effect was observed for *E. coli* on the bare FTO glass slides and randomly-coated FeOOH pillar particles on FTO glass (Figure 2c). Comparing the results between the FeOOH nanopillar arrays and randomly-coated FeOOH pillar particles on FTO glass, it is clear that the eradication of *E. coli* was achieved by the FeOOH nanopillars array structure. To prove this further, the LIVE/DEAD assay was used to observe the antibacterial properties of FeOOH nanopillar arrays surface. Red color indicates the bacteria were killed on the surface. SEM image in Figure 2e further confirmed that the killing of bacteria was due to surface rupture where bacteria were pierced by the pillars.

Since we have FeOOH surface with different morphology and different aspect ratio, the antibacterial property on different morphology of FeOOH surface has been evaluated. As shown in Figure 3, 1/3 length of FeOOH nanopillars array on glass and pyramid-shaped FeOOH array on glass don't showed antibacterial property. However, FeOOH nanopillars array prepared with two-step method showed equally good antibacterial property as the one-step method (Figure 2), with no colonies left after 24 h incubation. This experiment proved that the aspect ratio are well co-related to their antibacterial property.

Besides *E. coli*, which is an example of gram-negative bacteria (Figure 2c), *S. aureus* and *C. albicans*—representing gram-positive bacteria and fungi respectively—were also tested by the JIS method. As shown in Figure 4, both microbes were killed after a 24 h incubation, while cells on the bare FTO glass continued to grow. This indicates the FeOOH nanopillars array surface has good antimicrobial properties against different type of microbes.

The JIS testing method involved applying bacteria in nutrient broth on the testing surface, culturing at their desired growing conditions and counting the remaining bacteria after 24 h of incubation using the colony count method. During this test the solution remained on the testing surface and covered by a thin polystyrene film to prevent evaporation. We have also tested the structure-based antimicrobial effect by a droplet method.[36] In this method, a small drop of bacteria in PBS buffer solution (2.5 μl) was applied onto the testing surface, the water was allowed to evaporate which will impose additional force on bacteria against the tips of the nanopillars surface. As shown in Figure S7, after only 10 mins, all the bacteria (*E. coli* and *S. aureus)* on the surface were killed, while the number of bacteria on the bare glass control remained unchanged even after 15 mins.

The FeOOH nanopillars surface can be further converted to Fe_2O_3 nanopillars surface by calcination and annealed at 500 °C and 800 °C respectively.[46, 47] As shown in Figure S8, there is a significant color change from yellowish to dark red after calcinations, indicating the formation of α-Fe_2O_3 (hematite). XRD confirmed the transformation of FeOOH to α-Fe_2O_3 (Figure S8). SEM images in Figure 5 showed that at 500 °C, the FeOOH has transformed to α-Fe_2O_3, with nanopillar array structure well-preserved. However, at 800 °C, the nanopillars melted and the nanostructure surface was destroyed. Therefore, 500 °C was selected as the desired annealing condition and the antibacterial property was evaluated. For the annealed samples, all bacteria (*E. coli*) were killed after 24 h. This was also confirmed by SEM image in Figure 5c, and LIVE/DEAD results in Figure 5d.

3.3 Biocompatibility test

So far, we have demonstrated the preparation of FeOOH and Fe_2O_3 nanopillar array surfaces, both of which exhibit good antimicrobial properties. The good performance suggests they may have many potential applications. For *in vivo* applications, safety is a major concern. Since the antimicrobial property comes from the rupture effect by its structure, the same structure may destroy mammalian cells as well. To test this, biocompatibility of the nanostructured surface was carried out using the MTT method.[48] Mouse fibroblast cells were cultured on the FeOOH and Fe_2O_3 nanopillars array surfaces, and bare glass slides were used as control. As showed in Figure 6a, there is no significant viability difference between the nanostructured surfaces and the control, with cell viability close to that of the control (100%). Cell microscopic images also showed that cells proliferate very well on the nanostructure surfaces after 24 h, as compared to blank glass slides. This further confirmed that FeOOH and Fe_2O_3 nanopillars array surfaces have no cytotoxic effect on mouse fibroblast cells, which suggests that these surfaces are non-toxic and biocompatible with mammalian cells.

3.4 Sea urchin-type antibacterial coatings

During the preparation of the nanopillars surface, besides FeOOH nanopillars growing on the substrates, sea urchin-like FeOOH particles were also formed in the solution. Each pillar on the urchin-like particle is almost the same as the nanopillar growing on the surface. Therefore, the reaction conditions for the formation of sea urchin-type FeOOH were further optimized. As shown in Figure S9, highly robust urchin-like particles was formed with longer reaction time. The reaction at 100 °C for 24 h can form very robust FeOOH sea urchin-like particles, as shown in Figure 7 and Figure S9. By a simple heat treatment at 500 °C, FeOOH urchin-like particles can be converted to Fe_2O_3 urchin-like particles with an obvious color change from yellowish to dark red.

The sea urchin-like particles are self-standing. By simply coating the sea urchin-like powder onto the surface, self-standing urchin-like particles will automatically form a nanostructured surface, with nearly half of the urchin pillars poking upwards. We hypothesized that this self-standing nanopillars surface may have similar antimicrobial properties as the nanopillars array surface, as suggested in Figure 7a. To prove this, on 2.5 cm × 2.5 cm glass slides, 2.3 mg FeOOH or 1.9 mg Fe_2O_3 urchin-like particles were well dispersed in 100 µl ethanol and dropped onto the surface. After drying, a urchin coating was formed on the glass , as shown in Figure 7f-g. The amount of powder was determined based on the weight of the nanopillars array that grew on a glass substrate of the same size. Glass slides coated with equal amount of grinded urchin powders were used as control. The urchin-like particles were grinded using mortar to destroy the original urchin structure. SEM images of FeOOH and Fe_2O_3 were shown in Figure 7b and 7c. The antibacterial properties of the coatings were evaluated with the JIS Z 2801 method, as shown in Figure 7d and 7e. On FeOOH and Fe_2O_3 urchin-like surfaces, all the *E. Coli* were killed, whereas on grinded particles surfaces, there is no antibacterial activity. This proved that the FeOOH and Fe_2O_3 urchin-like coatings can be used as structure-based antibacterial coatings.

The coating of urchin-like particles is simply achieved by applying the powder suspension in ethanol onto the testing surface. As there are no binders, the coating is not strong and robust enough to resist washing. To solve this problem, aqueous-based polyacrylic acid paint was introduced as a binder. Initially, we mixed the non-diluted paint with the urchin-like powder, and coated onto the testing glass slide. However, JIS testing results showed that this surface has no antibacterial properties (Figure S10, c-d). SEM image showed that by mixing with non-diluted paint, the urchin-like particles were fully immersed in the paint matrix with no nanopillar structures exposed on the surface, and thus no antibacterial property was detected. Therefore, the paint was diluted 5 times with water and mixed with the urchin-like powder. This diluted solution was then coated onto the glass slides and showed good antibacterial property using the JIS testing method (Figure S10, a-b). The adhesive force of the coatings was measured following the ISO 2409 standard and the testing score is 5 (cannot be classified). Stronger binder may be considered in future work.

Compared to the nanopillar array surfaces, the sea urchin-like FeOOH and Fe_2O_3 coated surfaces are easier to apply, and they can be applied onto large surfaces and irregular surfaces as well. This provides a general method to form a killed-by-structure antimicrobial surface. Furthermore, FeOOH has an appealing yellowish color and Fe_2O_3 has a beautiful red hue (Figure 7, f-g). These painted surfaces may find useful applications in public areas such as hospitals, households, and transportation vehicles.

4. Conclusions

In summary, iron-based nanopillar array surfaces have been prepared by a solution-based hydrothermal method. The nanopillar arrays can grow on various substrates, and they showed good antibacterial properties. In addition, an even simpler method using sea urchin-type particles were proposed as self-standing particles to form nanostructured antimicrobial surfaces. These particles can easily formed nanostructured surfaces through coating and displayed equally good antibacterial properties. This method paves the way for the real applications of structure-based surface disinfection in daily life.

Conflicts of interest

There are no conflicts to declare.

Acknowledgements

This work was supported by the Institute of Bioengineering and Nanotechnology, Biomedical Research Council, Agency for Science, Technology and Research, and National Research Foundation (NRF), the Prime Minister's Office, Singapore under its NRF Competitive Research Program (NRF-CRP19-2017-02).

References

1. E. Banin, D. Hughes and O. P. Kuipers, *FEMS Microbiol. Rev.*, 2017, **41**, 450-452.
2. WHO, *Antimicrobial resistance: global report on surveillance 2014*, 2014.
3. K.-P. Koller, *Angew. Chem. Int. Ed.*, 2014, **53**, 3062-3062.
4. A. B. A. Boxall, *EMBO reports*, 2004, **5**, 1110-1116.
5. A. Alghamdi, S. Abdelmalek, A. Ashshi, H. Faidah, H. Shukri and A. Jiman-Fatani, *Afr. J. Microbiol. Res.*, 2011, **523**, 3998-4003.
6. Y. Wang, Y. N. Yang, Y. R. Shi, H. Song and C. Z. Yu, *Adv. Mater.*, DOI: 10.1002/adma.201904106, 21.
7. C. Mas-Moruno, B. Su and M. J. Dalby, *Adv. Healthc. Mater.*, 2019, **8**, 26.
8. J. Hasan, R. J. Crawford and E. P. Ivanova, *Trends Biotechnol.*, 2013, **31**, 295-304.
9. M. P. Muller, C. MacDougall and M. Lim, *J. Hosp. Infect.*, 2016, **92**, 7-13.
10. A. Elbourne, R. J. Crawford and E. P. Ivanova, *J. Colloid Interface Sci.*, 2017, **508**, 603-616.

11. G. V. Vimbela, S. M. Ngo, C. Fraze, L. Yang and D. A. Stout, *Int J Nanomedicine*, 2017, **12**, 3941-3965.
12. A. J. Scardino and R. de Nys, *Biofouling*, 2011, **27**, 73-86.
13. K. Liu and L. Jiang, *Nano Today*, 2011, **6**, 155-175.
14. S. Wu, B. Zhang, Y. Liu, X. Suo and H. Li, *Biointerphases*, 2018, **13**, 060801.
15. C. M. Magin, S. P. Cooper and A. B. Brennan, *Mater. Today*, 2010, **13**, 36-44.
16. G. Yi, S. N. Riduan, Y. Yuan and Y. Zhang, *Crit. Rev. Biotechnol.*, 2019, **39**, 964-979.
17. E. P. Ivanova, J. Hasan, H. K. Webb, V. K. Truong, G. S. Watson, J. A. Watson, V. A. Baulin, S. Pogodin, J. Y. Wang, M. J. Tobin, C. Lobbe and R. J. Crawford, *Small*, 2012, **8**, 2489-2494.
18. D. L. Gonzalez Arellano, K. W. Kolewe, V. K. Champagne, I. S. Kurtz, E. K. Burnett, J. A. Zakashansky, F. D. Arisoy, A. L. Briseno and J. D. Schiffman, *Sci. Rep.*, 2018, **8**, 11618.
19. C. D. Bandara, S. Singh, I. O. Afara, A. Wolff, T. Tesfamichael, K. Ostrikov and A. Oloyede, *ACS Appl. Mater. Inter.*, 2017, **9**, 6746-6760.
20. S. Pogodin, J. Hasan, V. A. Baulin, H. K. Webb, V. K. Truong, T. H. P. Nguyen, V. Boshkovikj, C. J. Fluke, G. S. Watson, J. A. Watson, R. J. Crawford and E. P. Ivanova, *Biophys. J.*, 2013, **104**, 835-840.
21. X. Li, *PCCP*, 2016, **18**, 1311-1316.
22. J. Jenkins, J. Mantell, C. Neal, A. Gholinia, P. Verkade, A. H. Nobbs and B. Su, *Nat. Commun.*, 2020, **11**, 14.
23. S. Venkataraman, A. L. Z. Lee, J. P. K. Tan, Y. C. Ng, A. L. Y. Lin, J. Y. K. Yong, G. Yi, Y. Zhang, I. J. Lim, T. T. Phan and Y. Y. Yang, *Polym. Chem.*, 2019, **10**, 412-423.
24. E. P. Ivanova, J. Hasan, H. K. Webb, G. Gervinskas, S. Juodkazis, V. K. Truong, A. H. F. Wu, R. N. Lamb, V. A. Baulin and G. S. Watson, *Nat. Commun.*, 2013, **4**, 2838.
25. T. Diu, N. Faruqui, T. Sjostrom, B. Lamarre, H. F. Jenkinson, B. Su and M. G. Ryadnov, *Sci. Rep.*, 2014, **4**, 7122.
26. G. Hazell, L. E. Fisher, W. A. Murray, A. H. Nobbs and B. Su, *J. Colloid Interface Sci.*, 2018, **528**, 389-399.
27. K. H. Tsui, X. Li, J. K. H. Tsoi, S. F. Leung, T. Lei, W. Y. Chak, C. F. Zhang, J. Chen, G. S. P. Cheung and Z. Y. Fan, *Nanoscale*, 2018, **10**, 10436-10442.
28. Q. F. Pan, Y. Cao, W. Xue, D. H. Zhu and W. W. Liu, *Langmuir*, 2019, **35**, 11414-11421.
29. E. P. Ivanova, D. P. Linklater, M. Werner, V. A. Baulin, X. Xu, N. Vrancken, S. Rubanov, E. Hanssen, J. Wandiyanto, V. K. Truong, A. Elbourne, S. Maclaughlin, S. Juodkazis and R. J. Crawford, *Proceedings of the National Academy of Sciences*, 2020, **117**, 12598-12605.
30. S. K. Saini, M. Halder, Y. Singh and R. V. Nair, *ACS Biomaterials Science & Engineering*, 2020, **6**, 2778-2786.
31. M. Michalska, F. Gambacorta, R. Divan, I. S. Aranson, A. Sokolov, P. Noirot and P. D. Laible, *Nanoscale*, 2018, **10**, 6639-6650.
32. J. Jenkins, J. Mantell, C. Neal, A. Gholinia, P. Verkade, A. H. Nobbs and B. Su, *Nat. Commun.*, 2020, **11**, 1626.
33. K. Kapat, P. P. Maity, A. P. Rameshbabu, P. K. Srivas, P. Majumdar and S. Dhara, *Journal of Materials Chemistry B*, 2018, **6**, 2877-2893.
34. G. Yi, Y. Yuan, X. Li and Y. Zhang, *Small*, 2018, **14**, e1703159.
35. Y. Xie, X. Qu, J. Li, D. Li, W. Wei, D. Hui, Q. Zhang, F. Meng, H. Yin, X. Xu, Y. Wang, L. Wang and Z. Zhou, *Sci. Total Environ.*, 2020, **738**, 139714.
36. M. Yamada, K. Minoura, T. Mizoguchi, K. Nakamatsu, T. Taguchi, T. Kameda, M. Sekiguchi, T. Suzutani and S. Konno, *PLoS One*, 2018, **13**.
37. S. M. Wu, F. Zuber, K. Maniura-Weber, J. Brugger and Q. Ren, *Journal of Nanobiotechnology*, 2018, **16**.
38. Y. Yuan and Y. G. Zhang, *Nanomed-nanotechnol.*, 2017, **13**, 2199-2207.
39. S. Wu, F. Zuber, J. Brugger, K. Maniura-Weber and Q. Ren, *Nanoscale*, 2016, **8**, 2620-2625.
40. Y. Jang, W. T. Choi, C. T. Johnson, A. J. Garcia, P. M. Singh, V. Breedveld, D. W. Hess and J. A. Champion, *Acs Biomaterials Science & Engineering*, 2018, **4**, 90-97.
41. C. Klein, *Manual of mineralogy (after James D. Dana)*, 1978.
42. Y. Song, S. Qin, Y. Zhang, W. Gao and J. Liu, *J. Phys. Chem. C*, 2010, **114**, 21158-21164.
43. S. N. Beer Pal, Sharma; Rakesh, Kumar; Ashwani, Kumar, *Indian J. Materi. Sci.*, 2015, **2015**, 7.
44. D. P. Linklater, M. De Volder, V. A. Baulin, M. Werner, S. Jessl, M. Golozar, L. Maggini, S. Rubanov, E. Hanssen, S. Juodkazis and E. P. Ivanova, *Acs Nano*, 2018, **12**, 6657-6667.
45. J. S. Association, *Journal*, 2001-08, 14.
46. K. Fan, F. Li, L. Wang, Q. Daniel, H. Chen, E. Gabrielsson, J. Sun and L. Sun, *ChemSusChem*, 2015, **8**, 3242-3247.
47. L. Yu, R. Han, X. Sang, J. Liu, M. P. Thomas, B. M. Hudak, A. Patel, K. Page and B. S. Guiton, *ACS Nano*, 2018, DOI: 10.1021/acsnano.8b02946.
48. S. Liu, R. J. Ono, H. Wu, J. Y. Teo, Z. C. Liang, K. Xu, M. Zhang, G. Zhong, J. P. K. Tan, M. Ng, C. Yang, J. Chan, Z. Ji, C. Bao, K. Kumar, S. Gao, A. Lee, M. Fevre, H. Dong, J. Y. Ying, L. Li, W. Fan, J. L. Hedrick and Y. Y. Yang, *Biomaterials*, 2017, **127**, 36-48.

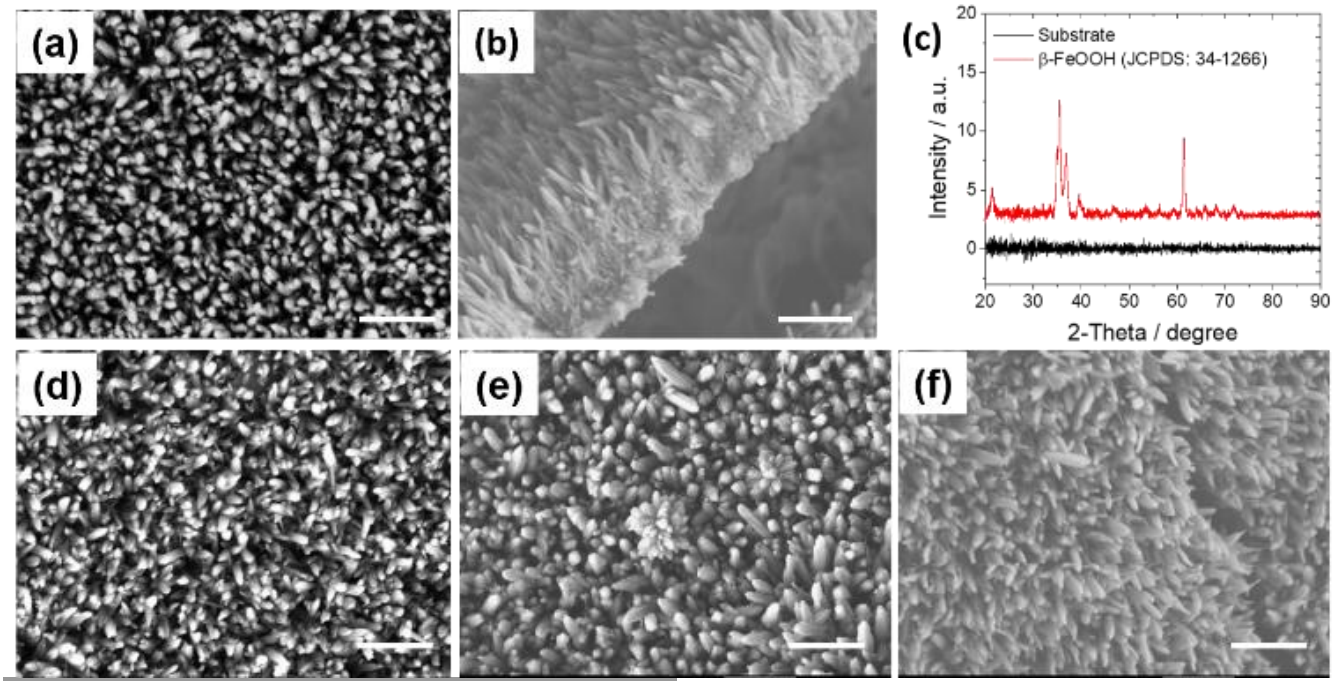

Fig. 1. SEM images of FeOOH nanopillar arrays growing on different substrate of (a-b) glass, (d) fluorine-doped tin oxide (FTO) glass, (e) tin-coated iron, (f) Teflon tape, and (c) X-ray diffraction pattern of β-FeOOH nanopillars on glass. Bar = 1 μm.

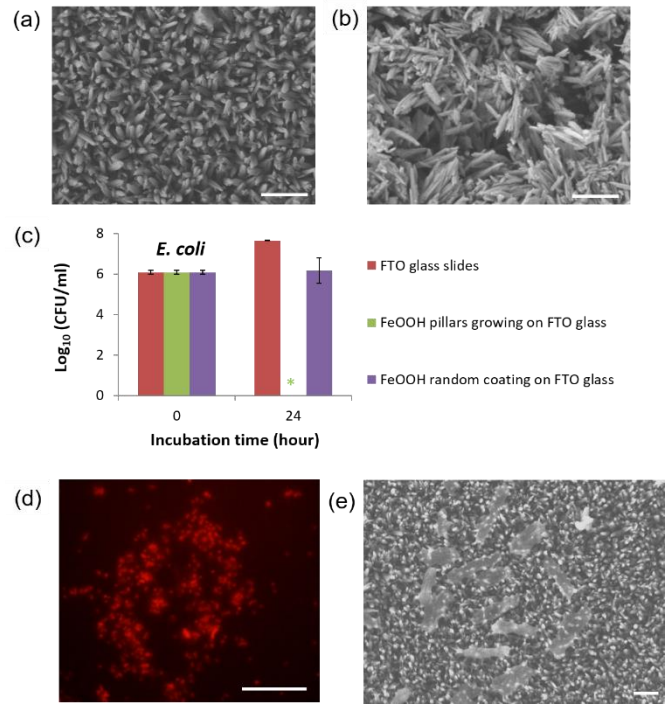

Fig. 2. Antibacterial properties of FeOOH nanopillars surface on FTO glass. (a) SEM image of FeOOH nanopillars array growing on FTO glass, and (b) SEM image of FeOOH pillar particles randomly-coated onto FTO glass. (c) antibacterial properties of the surface tested by JIS Z 2801/ISO 22196 method, (d) antibacterial properties of the nanopillars surface with LIVE/DEAD method, and (e) SEM image of *E. coli* killed on the nanopillars surface. * indicates that no colony was observed. The data are expressed as mean ± S.D. of triplicates. Bar = 1 μm for a, b, e, and bar=100 μm for d.

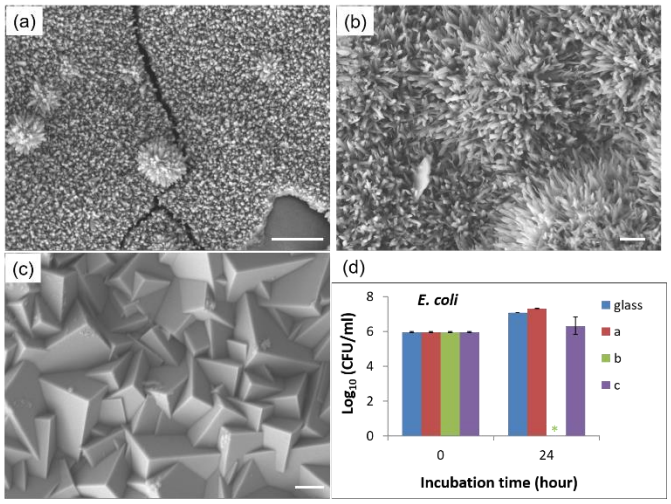

Fig. 3. Aspect ratio effect of FeOOH on their antibacterial properties. (a) SEM image of FeOOH nanopillars array with 1/3 length on glass, and (b) SEM image of FeOOH nanopillars prepared with 2-step method on glass. (c) FeOOH pyramid on glass, and (d) antibacterial properties of the surface tested by JIS Z 2801/ISO 22196 method. * indicates that no colony was observed. The data are expressed as mean ± S.D. of triplicates. Bar = 1 μm.

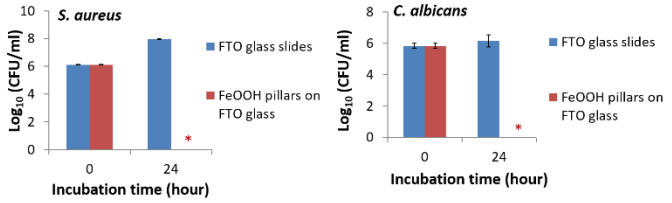

Fig. 4. Antimicrobial properties of the surface tested by JIS Z 2801/ISO 22196 method for (a) *S. aureus* and (b) *C. albicans*. * indicates that no colony was observed. The data are expressed as mean ± S.D. of triplicates.

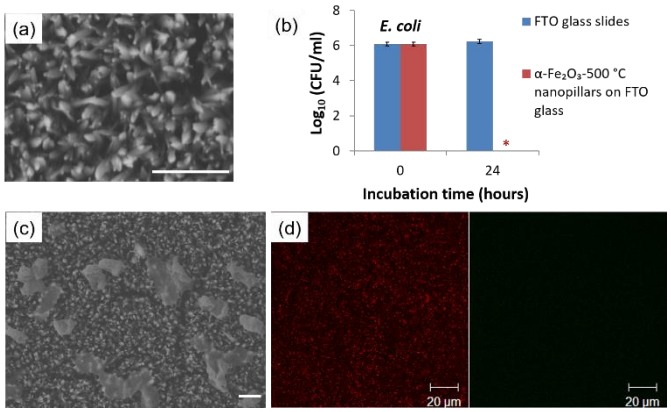

Fig. 5. SEM and antibacterial properties of α-Fe_2O_3 nanopillars surface on FTO glass. (a) SEM image of α-Fe_2O_3 nanopillars array on FTO glass, and (b) antibacterial properties of the surface tested by JIS Z 2801/ISO 22196 method, (c) SEM image of *E. coli* killed on the nanopillars surface, and (d) antibacterial properties of the nanopillars surface with LIVE/DEAD method. * indicates that no colony was observed. The data are expressed as mean ± S.D. of triplicates. Bar = 1 µm.

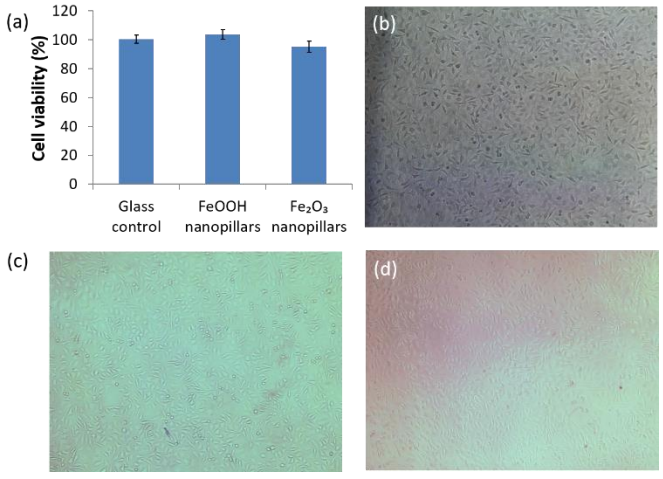

Fig. 6. Evaluation of biocompatibility. (a) Viability of mouse fibroblast cells after being cultured for 24 h on FeOOH and Fe_2O_3 nanopillars array surfaces in comparison with bare glass slides. (b-d) microscopic images of mammalian fibroblast cells growing on the three surfaces of (b) glass slide, (c) FeOOH nanopillars surface, and (d) Fe_2O_3 nanopillars array surface.

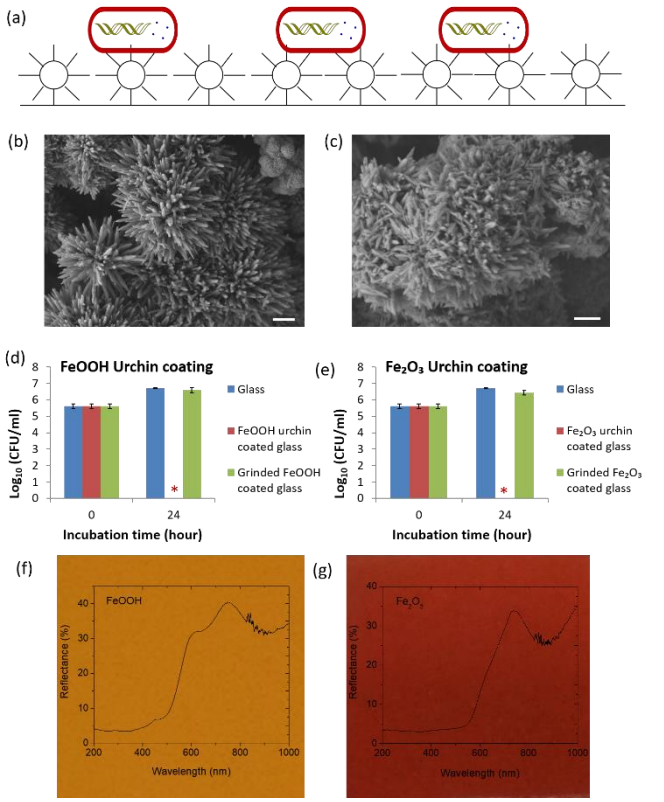

Fig. 7. (a) Schematic illustration of antimicrobial nanostructured surface formed by sea urchin-like particles. (b) sea urchin-like FeOOH particles and (c) Fe_2O_3 particles. JIS testing results for (d) FeOOH and (e) Fe_2O_3 coated surface. (f-g) Photograph of sea urchin-like (f) FeOOH and (g) Fe_2O_3 coated surface on glass, and their reflection spectra. Bar = 1 µm.

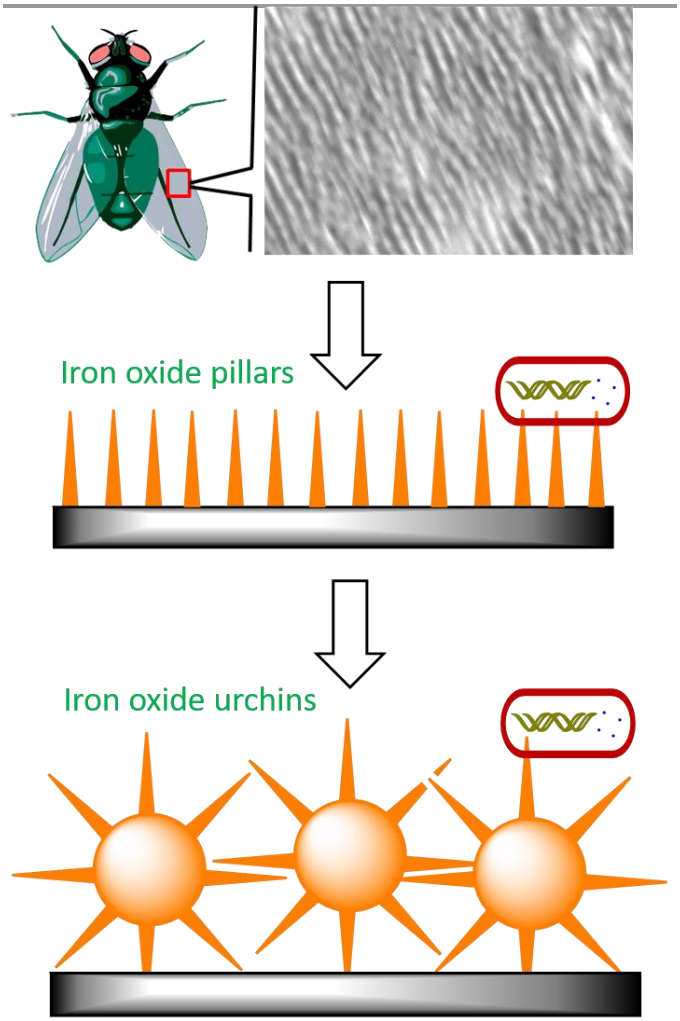

Table of Contents (TOC): Bactericidal nanopillar array surfaces of FeOOH and Fe_2O_3 have been prepared as a cicada wing mimicry using a simple solution method. An even simpler structure-based antimicrobial surface was also made by coating with sea urchin-like FeOOH and Fe_2O_3 particles. This method provides a general way to prepare structure-based antimicrobial surfaces for real applications.